

Supporting Information

Porphyrin-based Porous Organic Polymer for NIR-enhanced delivery of bupivacaine towards Pain management in bacteria infection therapy

Lichao Chu,^{a,b,#} Chunyu Dong,^{c,#} Shuai Wang,^b Xin Ding,^b Jingsong Yuan,^b Peilei Chen,^b Yanhua Luo,^{b*} Lingzhi Yu^{a*}

^a. *Jinan Central Hospital, Shandong University, Jinan, Shandong, PR China*

^b *Weifang People's Hospital, Shandong Second Medical University, Weifang 261035, Shandong, PR China*

^c. *Department of Neurointervention, Weihai Central Hospital Affiliated to Qingdao University, Weihai, Shandong, PR China*

#These authors contribute equal to this work.

* Correspondence authors

E-mail: pain-relief@163.com (L. Yu); 55358645@qq.com (Y. Luo)

Contents

Section 1. Experimental Section

Section 2. Methods

Section 3. Duration of analgesia in the hind legs of mice after subcutaneous injection

Section 4. NMR of P-POP-Bu

Section 5. PXR of P-POP-BU

Section 6. TG-DSC of P-POP-BU

Section 7. N₂ adsorption and desorption test and pore size distribution

Section 8. Degradation of P-POP under different conditions

Section 9. MTT assay and hemolysis test for P-POP-Bu

Section 10. UV absorption spectra and working curves of Bu in ethanol

Section 11. Working Curve of Bu in PBS and BU Release from P-POP-BU

Section 12. Supported Tables

Section 1. Experimental Section

1.1 Materials

All raw materials, including the solvents and reagents employed for the synthesis of the porous organic polymer and corresponding drug-loaded composite were provided by commercial suppliers, which were directly used without further purification unless otherwise stated. The pyrrole was temporarily redistilled before the applications. Luria Broth and Agar were purchased from Hopebio. Live&Dead Bacterial Staining Kit was purchased from YENSEN. MTT was purchased from Beyotime. Calcein-AM/PI Double Stain Kit was purchased from YENSEN. Paraformaldehyde (4%) was purchased from Biosharp Biotechnology.

1.2 Synthesis of 1,1'-Ferrocenedicarboxaldehyde

Ferrocene (1.86 g, 10 mmol) was accurately weighed, which was added into a 250 mL three-necked flask with a magnet. Then, hexane (75 mL) and TMEDA (8 mL) were added into the reaction system which was then degassed and fulfilled with argon. The three-necked flask was placed in a cryostat at -78 °C and stirred well at 300 rpm for 10 minutes, then a hexane solution (9 mL) of n-BuLi (2.5 M) was added. The reaction system was gradually brought to room temperature, which was kept for 12 h to give an orange-red solid. The orange-red solid was then washed with hexane (50 mL) at room temperature and dispersed in 50 mL of hexane containing 3.6 mL of DMF and 15 mL of THF. Under continuously stirring for 10 min, 30 mL (14%) hydrochloric acid was added to the above solution to produce a red solid. The red solid was washed with hexane (50 mL), and the aqueous phase was extracted with dichloromethane (50 mL). The organic phases were combined and distilled under reduced pressure to give a red crystalline crude. The red crystals were purified by silica gel column to obtain purer red crystals (yield: 1.50 g, 62%). ¹H-NMR (400 MHz, CDCl₃): δ = 9.88 (s, 2H), 4.82 (s, 4H), 4.61 (s, 4H).

1.3 Synthesis of 5,10,15,20-tetrakis(4-cyanophenyl)porphyrin

4-Cyanobenzaldehyde (7.5 g, 10.5 mmol) and propionic acid (200 mL) were added to a 250 mL three-necked flask with a magnet. The flask was heated to reflux for 3 h at 300 rpm. Then, redistilled pyrrole (5.19 mL, 75 mmol) was added into the reaction

mixture, and the reaction was maintained for 1 h. After 1 h, the reaction mixture was cooled to 27 °C, poured into MeOH (250 mL), and stirred in an ice bath for 30 min. After 30 min, the blackish-purple solids on the filter cake were collected by filtration and the filtered cake was washed again with MeOH until the filtrate became clear. Subsequently, the solid was washed with warm distilled water and the obtained solid was purified by silica gel column. The purified product was dried in a vacuum drying oven at 70 °C for 12 h to give a black-purple solid (Yield: 1.10 g, 58.8%). ¹H-NMR (400 MHz, CDCl₃): δ = 8.73 (s, 8H); 8.26 (d, *J* = 7.60 Hz, 8H); 8.03 (d, *J* = 7.60 Hz, 8H).

1.4 Synthesis of 5,10,15,20-tetrakis(4-(2,4-diaminotriazine)phenyl)porphyrin

5,10,15,20-tetrakis(4-cyanophenyl)porphyrin (879 mg, 1.23 mmol), dicyandiamide (571.5 mg, 6.15 mmol) and KOH (450 mg, 7.95 mmol) were added to a 150 mL three-neck round bottom flask with magnets. After degassing and back-filled with argon, dry 2-methoxyethanol (30 mL) was added to the reaction system. And the reaction system was heated to reflux at 300 rpm for 48 h. The product was then washed with warm distilled water (150 mL) and dried in a vacuum oven at 70 °C for 8-12 h to give a black-purple solid (yield: 1.11 g, 86%). ¹H-NMR (400 MHz, DMSO-d₆): δ = 8.93 (s, 8H), 8.70 (d, *J* = 7.60 Hz, 8H), 8.34 (d, *J* = 7.60 Hz, 8H), 6.92 (s, 16H).

1.5 Synthesis of P-POP

1,1'-ferrocenedicarboxaldehyde (Fc) (1.45 g, 6.0 mmol) and 5,10,15,20-tetrakis(4-(2,4-diaminotriazine)phenyl)porphyrin (TDPP) (0.79 g, 0.75 mmol) were added to an autoclave (50 mL) containing dimethyl sulfoxide (20 mL). The reaction mixture was heated to 180 °C and kept for 40 h. During this process, a black solid is formed. The reaction mixture was then naturally cooled to room temperature. The solid was separated by filtration to obtain black solid, which was washed with methanol, DMF and THF until the filtrate was colorless. The resulting black solid was dried in a vacuum oven at 120 °C overnight to obtain a black fluffy powder (2.12 g, yield: 95%).

1.6 Synthesis of P-POP-BU

3 mg each of P-POP powder and bupivacaine (BU) powder were weighed into a 5 mL brown flat-bottomed vial with a small magnet, and 3 mL of anhydrous ethanol was

added and mixed at 500 rpm for 12 h. After 12 h, the solvent was filtered to obtain the black powder P-POP-BU.

Section 2. Methods

2.1 Material characterization

The ^1H -NMR and ^{13}C CP/MAS NMR spectra of the prepared monomers were recorded on Avance Bruker DPX 400 (400 MHz). Fourier transform infrared (FT-IR) spectroscopy was performed on mixed powder of target substance and KBr using Spectrum Spotlingt 400 in the range of 4000 to 400 cm^{-1} . The morphology of the powder samples was evaluated by field emission scanning electron microscopy (SEM, Ultra 55) and transmission electron microscopy (TEM, Tecnai G2 20 TWIN) by dipping the prepared samples on a copper grid. N_2 adsorption and desorption measurements were carried out on a Belsorp max analyzer (Japan) at a low temperature of 77 K. Prior to testing, all these samples were degassed overnight at 150°C under high vacuum to remove solvent or water absorbed in the porous skeleton. Thermogravimetric analysis (TGA) was recorded with a microcomputer differential thermal equilibrium (HCT-1, Hengjiu, Beijing, China) analyzer under the protection of N_2 . UV-Vis spectra of samples were obtained by a Shimadzu UV 2600 spectrophotometer (Shimadzu, Japan) in the range of 200 nm to 800 nm. Powder X-ray diffraction (PXRD) parameters were obtained with a Rigaku-DMAX 2500 diffractometer from 5° to 80° at 6° min^{-1} .

2.2 Photothermal performance test

1 mL of P-POP aqueous suspensions at concentrations of 0, 50, 100, 200, 400, and 600 $\mu\text{g mL}^{-1}$ were added to a 1.5 mL EP tube and then irradiated with 808 nm laser at a power density of 1.5 W cm^{-2} for 10 min at room temperature. Meanwhile, P-POP-BU at a concentration of 400 $\mu\text{g mL}^{-1}$ was irradiated with an 808 nm laser at power densities of 1.0, 1.5 and 2.0 W cm^{-2} for 10 min at ambient P-POP-BU temperature. Temperature changes during irradiation were monitored using an infrared thermographic camera, and images of temperature changes at different time points were taken. The photothermal stability of P-POP-BU was then evaluated by ON/OFF cyclic irradiation experiments. Briefly, 1 mL of 400 $\mu\text{g mL}^{-1}$ of P-POP-BU aqueous

suspension was first irradiated with 808 nm laser for 10 min at room temperature. The laser was then turned off and P-POP-BU was naturally cooled to the starting temperature at room temperature. Four laser cycles were repeated in the same manner. Temperature changes were recorded throughout the experiment.

2.3 Calculation of photothermal conversion efficiency

The aqueous dispersion system of P-POP-BU is irradiated using red light ($\lambda = 808$ nm, 1.5 W cm^{-2}) for 10 min at room temperature. Then, the aqueous dispersion system of the heated P-POP was waited to cool naturally at ambient temperature, and both the heating and cooling processes were monitored in real time using a thermometer with a thermocouple probe. The photothermal conversion efficiency (η) is calculated by the following equation:

$$\eta (\%) = [hS(T_{\max} - T_{\text{surr}}) - Q_{\text{dis}}] / I(1 - 10^{-A_{808}}) \quad (\text{S1})$$

The meaning of each element in the formula is given as follows: ‘h’ is the heat transfer coefficient; ‘S’ is the surface area of the vessel; ‘ T_{\max} ’ is the equilibrium temperature after 10 minutes of irradiation (53.6°C); ‘ T_{surr} ’ is the ambient temperature at the time of the experiment (25.9°C); ‘ Q_{dis} ’ is the heat dissipation of the test cell (25.03 mW); ‘I’ represents the laser power at 808 nm (1.5 W cm^{-2}). ‘ A_{808} ’ is the absorbance of P-POP-BU aqueous solution at 808 nm (0.368).

$$hS = m_{\text{H}_2\text{O}} C_{\text{H}_2\text{O}} / \tau S \quad (\text{S2})$$

$$t = -\tau S (\ln \theta) \quad (\text{S3})$$

The meanings of each element in the formula are also listed: ‘ $m_{\text{H}_2\text{O}}$ ’ referred to the mass of water solvent ($1 \times 10^{-3} \text{ kg}$) at the time of experiment; ‘ $C_{\text{H}_2\text{O}}$ ’ represented the specific heat capacity of water ($4.2 \times 10^3 \text{ J/kg } ^\circ\text{C}$); ‘ τS ’ was the P-POP-BU time constant (254); ‘ θ ’ is the ratio of ΔT and T_{Max} .

2.4 Pain management experiment

2.4.1 Selection of Animal Model

In this study, we used an animal model similar to that reported by Esad Ulker et al. A postoperative pain model was employed to reduce the pain threshold of mice. The surgical procedure was based on the protocol described by Esad Ulker et al. In this model, the incision procedure was performed according to the description by Cowie &

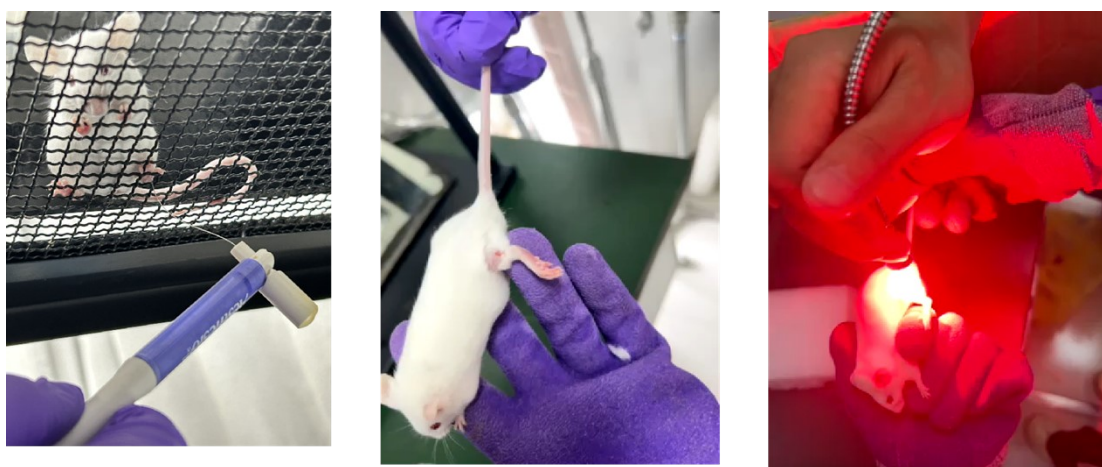
Stucky (2019). Mice were induced with 5.0% sevoflurane and anesthesia was maintained using a constant 2.5% sevoflurane concentration in oxygen via a mask and vaporizer. The surgical site was disinfected with iodophor. All surgeries were performed by the same experimenter (EU) to ensure consistency. All surgeries were conducted between 08:00 AM and 11:00 AM. The skin and fascia of the left hind paw were incised by 0.5 to 1.0 cm, and the muscle was separated longitudinally in the anteroposterior direction. The incision was sutured after 5 minutes, and the total duration of the surgery was between 7 and 10 minutes. After recovery from anesthesia, the mice were returned to their housing cages to avoid anxiety caused by a new cage. Sham-operated groups corresponding to each surgical group received sevoflurane for the same duration and the surgical site was disinfected, but no incision was made.

The validation of this model primarily relied on changes in mechanical pain threshold. With the successful establishment of the model, the mechanical pain threshold of mice decreased.

The adjusted paw withdrawal model was used to assess sensation, which responded to graded stimuli using von Frey filaments. A metal mesh platform (1.25 cm mesh) surface was divided into 15 cm × 10 cm × 10 cm compartments using plexiglass dividers. Each mouse was placed in a separate compartment and allowed to adapt to the environment for 5-10 minutes. After the animal rested, the von Frey filaments were used to test the baseline sensation of the intact plantar surface of the left hind paw. Each filament produced a specific reproducible force, and each filament was applied perpendicularly to the paw with sufficient force to cause slight bending and held for 2 to 3 seconds. Graded stimulus testing was performed by applying two stimuli of the same intensity to the hind paw at intervals of several seconds. The test started with a filament producing a force of 0.02 g and increased sequentially to a filament producing a force of 2.0 g. Studies have shown that in all cases, a force of 2.0 g is sufficient to lift the hind paw off the platform. The sensory test was terminated when paw withdrawal occurred or when the animal did not withdraw in response to the maximum force of the test. Baseline tests were performed on the surgical and sham-operated groups at 5-minute intervals on the surgical paw. The test results indicated that postoperative mice

had increased pain sensitivity, and the pain threshold reached the lowest level on the first postoperative day. As time passed, the wound gradually recovered, and the pain threshold of the surgical group gradually returned to the level of the control group. Therefore, mice on the first postoperative day were selected as the pain sensitivity model for the study of light-controlled analgesic performance.

The validation of this model primarily relied on changes in mechanical pain threshold. With the successful establishment of the model, the mechanical pain threshold of mice decreased.



Scheme S1. Modeling and experimental equipment: animal anesthesia machine, vonferly ciliary mechanical stimulation needle metal mesh platform and compartment.

2.4.2 Study of Light-Controlled Analgesic Performance

Sixty postoperative mice (n=6 per group) were divided into 10 groups. The experimental design included the following groups: BU, P-POP-BU group, P-POP-BU light exposure group, P-POP group. After anesthesia with sevoflurane, a 1 mL syringe was used to subcutaneously inject 0.5% BU, P-POP-BU (200 $\mu\text{g}/\text{mL}$), P-POP (200 $\mu\text{g}/\text{mL}$), or 20 μL of saline into the incision site on the left hind paw according to the experimental grouping. The groups requiring light exposure were irradiated with NIR (808 nm, 1.0 W/cm^2) at the subcutaneous injection site for 2 minutes after injection.

After all group treatments were completed, the mice were placed in plexiglass compartments on the metal mesh platform and allowed to stabilize before pain testing. The saline group and the saline light exposure group were used as control groups to compare the changes in postoperative pain threshold with the two composite materials.

Apart from examining the differences in pain threshold changes, the duration of analgesia was compared based on the drug release characteristics of each group. The duration of analgesia was the time from subcutaneous injection to the last test interval during which no withdrawal occurred in response to a force of 0.07 g. Meanwhile, according to the light-controlled drug release characteristics of the composite materials, NIR irradiation (808 nm, 1.0 W cm⁻²) was applied to the two composite materials at 12-h intervals to compare the attenuation of analgesic duration.

2.5 Antibacterial Capability Test

Individual colonies of *E. coli* and *S. aureus*, used as Gram-negative and Gram-positive bacterial models, respectively, were transferred to 5 mL of Luria-Bertani (LB) medium (containing trypsin 10 g/L, yeast extract 5 g/L, NaCl 10 g/L, pH=7.4) and grown in an incubator at 110 rpm at 37 °C for 12 h. The fresh strains were diluted with phosphate buffered saline (PBS, pH=7.3) to dilute the fresh strain in LB medium to obtain the desired concentration (OD₆₀₀=0.15, equivalent to 1 × 10⁸ CFU/mL).

2.6 Determination of antimicrobial properties of P-POP-BU

900 mL of P-POP-BU at different concentrations (100, 200, 400 µg mL⁻¹) was laser irradiated with *S. aureus* and *E. coli* (100 µL, 1 × 10⁸ CFU mL⁻¹) for 10 min (λ = 808 nm, 1.5 W cm⁻²) and co-cultivated for 12 h at 37°C. After gradient dilution, 80 µL of bacteria were transferred to solid medium, and the antimicrobial activity of different concentrations of P-POP-BU was estimated by plate counting method, and all experiments were repeated three times. In addition, 900 mL of the same concentration (400 µg mL⁻¹) of P-POP, BU, P-POP-BU (400 µg mL⁻¹) were treated with *S. aureus* and *E. coli* (100 µL, 1 × 10⁸ CFU mL⁻¹) with or without laser irradiation (λ = 808 nm, 1.5 W cm⁻², 10 min) treatments and then co-cultivated at 37°C for 12 h. After gradient dilution, 80 µL of bacteria were transferred to solid medium, and the antimicrobial activity of P-POP-BU under different conditions was estimated by plate counting method, and all experiments were repeated three times.

2.7 Live/dead staining of bacteria

DMAO and EthD-III are used to differentiate between live and dead microbial cells. DMAO penetrates all bacterial membranes (intact and damaged), labeling the

bacteria green, whereas EthD-III only penetrates damaged bacterial membranes, labeling the bacteria red and reducing the green color of DMAO. Specifically, 100 μL of *E. coli* or *S. aureus* (1×10^8 CFU) was incubated with 400 μL of PBS, 400 μL of BU, 400 μL of P-POP ($400 \mu\text{g mL}^{-1}$), and 400 μL of P-POP-BU ($400 \mu\text{g mL}^{-1}$) or 400 μL of PBS + laser, 400 μL BU + laser, 400 μL P-POP ($400 \mu\text{g mL}^{-1}$) + laser and 400 μL P-POP-BU ($400 \mu\text{g mL}^{-1}$) + laser incubation with 4 μL DMAO and 8 μL EthD-III at 37 °C for 10 min in the dark. After staining, 50 μL of the bacterial solution was placed on the surface of a slide. Images of *E. coli* or *S. aureus* were then captured using a fluorescent inverted microscope.

2.8 Transmission electron microscopy (TEM) of bacteria

Bacterial suspensions of different experimental groups were prepared according to the method in Determination of antimicrobial properties of P-POP-BU. Bacteria were fixed in 2.5% glutaraldehyde solution (4°C, 24 h), washed three times with PBS, embedded in agar and blocked. The bacteria were then dehydrated by continuous treatment with ethanol solutions (30%, 50%, 70%, 90%, 95% and 100%) for 10 minutes at room temperature, followed by treatment with acetone for 3 hours at room temperature, embedding by gradient infiltration of embedding medium, negative staining and sectioning on a nickel mesh. The nickel nets were placed under TEM observation. Their morphology was captured.

2.9 In vivo wound healing experiment

Wound healing was modeled using 5 to 6-week-old female KM mice (from Swiss mice) ($n = 5$ per group, 25-30 g) divided into 6 groups. After disinfection with ethanol solution (75%), the dorsal hair of each mouse was shaved prior to surgery to form a $d = 5$ mm wound, which was then infected with *Staphylococcus aureus* (1×10^8 CFU/mL) for 24 hours. The wound was then treated with PBS (50 μL), BU (50 μL) P-POP (50 μL , $400 \mu\text{g mL}^{-1}$), P-POP-BU (50 μL , $400 \mu\text{g mL}^{-1}$), P-POP + laser (50 μL , $400 \mu\text{g mL}^{-1}$) and P-POP-BU + laser (50 μL , $400 \mu\text{g mL}^{-1}$) treated infected wounds ($\lambda = 808$ nm, 1.5 W cm^{-2} for 10 min) and photographs were taken of the wound surfaces on days 1, 3, 5, 7, and 11 while the body weight of the mice was monitored. Changes in wound size were measured using an image analysis program (Image. J, National Institutes of

Health). All mice died on day 11. Wound skin tissue and major organs, including the heart, liver, spleen, lungs, and kidneys, were excised and fixed in 10% formalin, followed by H&E staining and Masson's trichrome staining. On day 11, 1 to 2 mL of blood samples were collected from the fundus arteriosus of the mouse. 200 μ L of each blood sample was taken for routine blood analysis, including WBC, RBC, HGB, HCT, MCV, MCHC, PLT and MCHC.

2.10 P-POP-BU degradation by reactive species

The degradation of P-POP-Bu in various pH solutions was evaluated using the subsequent procedures. Specifically, P-POP-Bu (2 mg) were introduced into 2 mL of diverse pH solutions. Following a 72-h incubation period, the mixtures were centrifuged, and the supernatant was subsequently analyzed to determine the UV absorption spectra within the solutions employing a UV-Vis spectrophotometer. Additionally, the degradation behavior of P-POP-Bu was investigated in the presence of hydroxyl radicals (\cdot OH). This was accomplished by incubating P-POP-Bu in solutions containing either 10 mM or 100 mM of H₂O₂, along with either 1 mM or 10 mM of FeSO₄, which were designated as 1 \times \cdot OH and 10 \times \cdot OH conditions, respectively.

2.11 Drug loading rate and encapsulation rate experiments of P-POP-BU

Ethanol solutions containing various concentrations of BU (50, 100, 150, 166, 200, 250, 300, 450, and 500 μ g/mL) were prepared. The absorbance of these solutions was measured using a UV-Vis spectrophotometer to establish the working curve. Following this, different standard profiles of BU solutions were created by combining 1 mL of P-POP-BU with 2, 4, 6, and 8 mg of BU in 2 milliliters of ethanol solution, respectively. These mixtures were stirred for 24 h. The residual quantity of BU in the supernatant was then determined using a UV-Vis spectrophotometer, employing the following equations:

$$\text{Loading rate LC\%} = (W_1 - W_2) / W_3 * 100\%$$

$$\text{Encapsulation rate EF\%} = (W_1 - W_2) / W_1 * 100\%$$

Where “W₁” is the mass of added drug, “W₂” is the mass of remaining drug, and “W₃” is the mass of drug carrier complex.

2.12 P-POP-Bu released in PBS

To establish the standard curve, a PBS solution with a pH of 7.4 was formulated containing various concentrations of BU: 0.3, 0.4, 0.5, 0.6, 0.7, 0.8, and 0.9 mg/mL. The absorbance of these solutions at a wavelength of 271 nm was then measured using a UV-Vis spectrophotometer.

For the assessment of BU release from P-POP-Bu, 2 mg of P-POP-BU were introduced into 3 mL of a PBS solution with a pH of 7.4. The absorbance of the solution was then monitored over time using a UV-Vis spectrophotometer.

2.13 P-POP-Bu hemolytic assay

Fresh blood was taken from KM female mice (derived from Swiss mice). Erythrocytes were collected by centrifugation at 10,000 rpm for 20 min and then washed three times with PBS. The erythrocytes (4% w/w) were then incubated with P-POP-Bu at a ratio of 1:9 (v/v) for 3 h at 37°C, followed by centrifugation at 12,000 rpm for 20 min. Then, 100 µL of supernatant from each group was placed in a 96-well plate and the absorbance of each group was measured at 570 nm using an enzyme marker. Distilled water was used as a positive control and PBS as a negative control. The amount of hemolysis was calculated using the following formula:

$$\text{Hemolysis (\%)} = (A - A_n) / (A_p - A_n) * 100\% \text{ (S4)}$$

Where "A" is the absorbance obtained by taking the supernatant after adding P-POP-Bu to the erythrocytes. "A_n" is the absorbance obtained by taking the supernatant after adding PBS to the red blood cells (negative control). "A_p" is the absorbance obtained by taking the supernatant after the addition of distilled water to the red cells (positive control).

2.14 MTT assay of P-POP-Bu

In 96-well plates, 3T3 cells were seeded at a density of 5×10^3 cells per well at 180 µL cells per well and liquid sealed by adding 200 µL PBS to surrounding duplicate wells to prevent excessive evaporation. After 24 h of incubation, 20 µL of the expanded tenfold concentration of the drug was added as per the grouping and concentration gradient of the *in vitro* antimicrobial assay and incubated together for 72 h in the presence or absence of laser irradiation ($\lambda = 808$ nm, 1.5 W/cm², 10 min). 20 µL of MTT (5 mg/mL) solution was then added to each well and incubated in the incubator

for 4 h. After 4 h, the supernatant was aspirated and 150 μ L of DMSO was added with the aim of dissolving the MTT-carboxamide crystals. After 10 min of dissolution on a shaker, the absorbance of the 96-well plates was measured at 570 nm using an enzyme marker. Each set of experiments was repeated three times.

2.15 Statistical analysis

All statistical analysis was conducted using GraphPad Prism 8.0 software. Statistical differences were determined using either a one-way or two-way ANOVA with a post hoc Tukey's test for multiple comparison. All data are presented as means \pm standard deviation (SD) and $p < 0.05$ was considered the level of significance. (* $p < 0.05$, ** $p < 0.01$, *** $p < 0.001$, **** $p < 0.0001$)

Section 3. Duration of analgesia in the hind legs of mice after subcutaneous injection

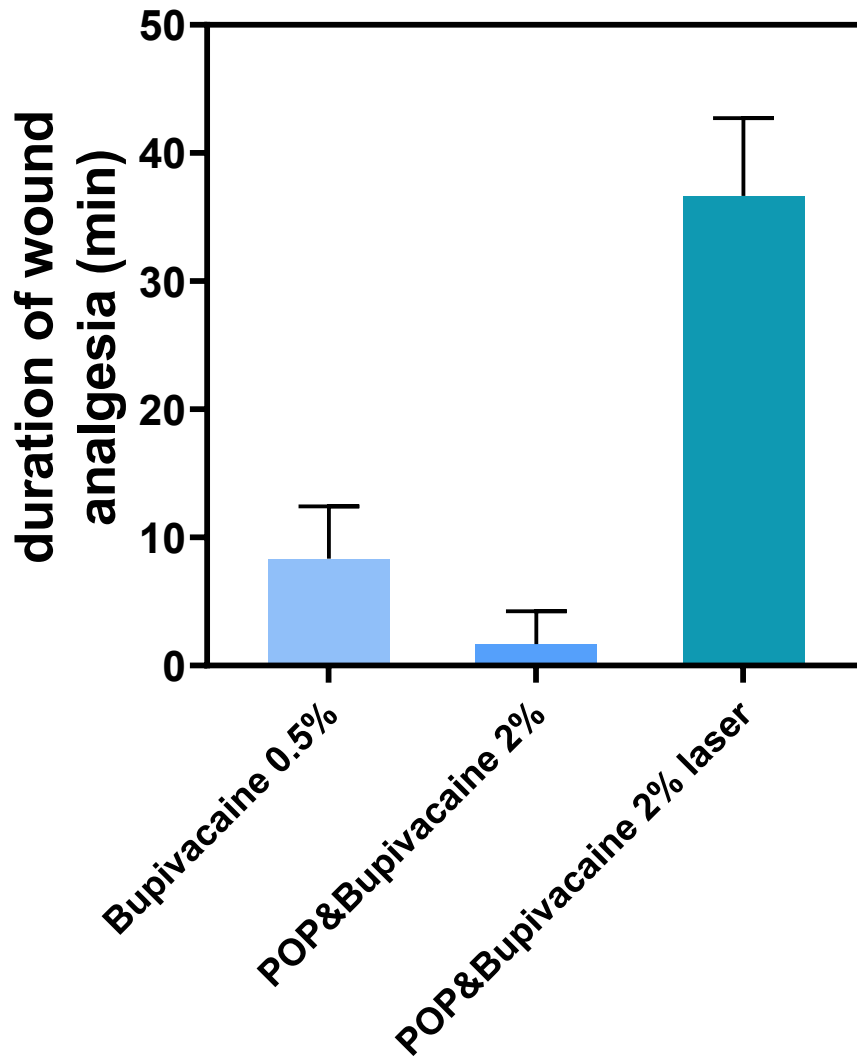


Figure S1. Duration of analgesia in the hind legs of mice after subcutaneous injection with 0.5% bupivacaine or POP loaded with 2% bupivacaine (mean SD)

Section 4. NMR of P-POP-Bu

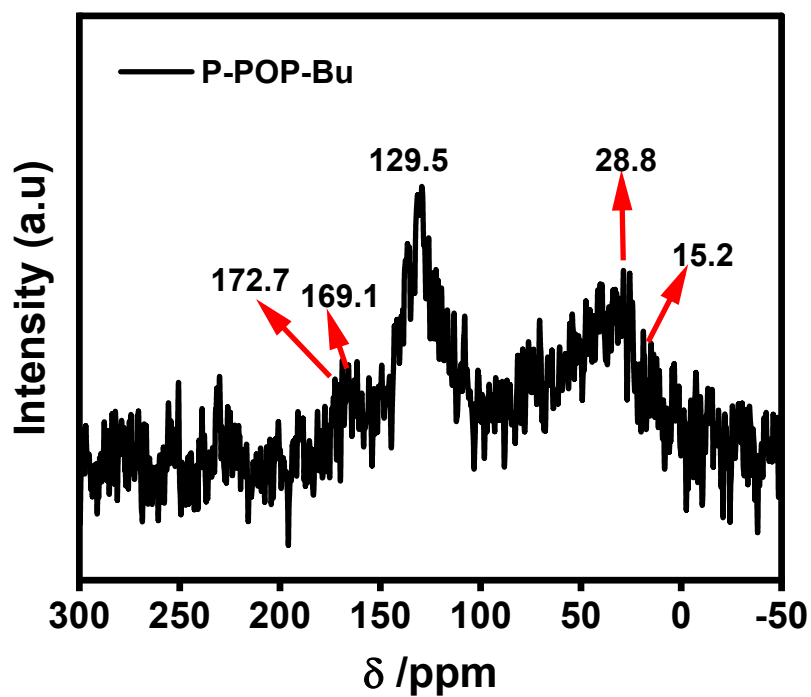


Figure S2. Solid-state NMR mapping of P-POP-BU

Section 5. PXRD of P-POP-BU

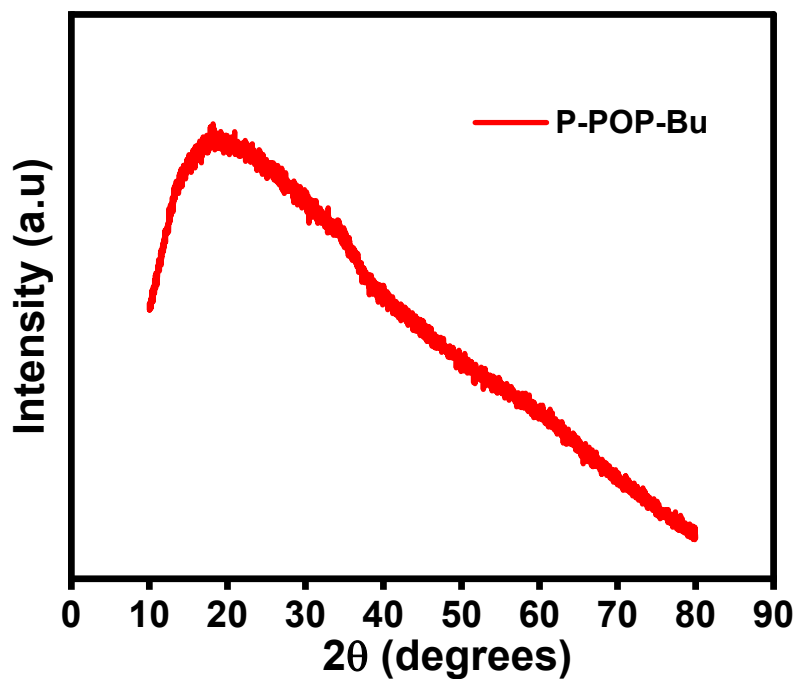


Figure S3. PXRD pattern of P-POP-BU

Section 6. TG-DSC of P-POP-BU

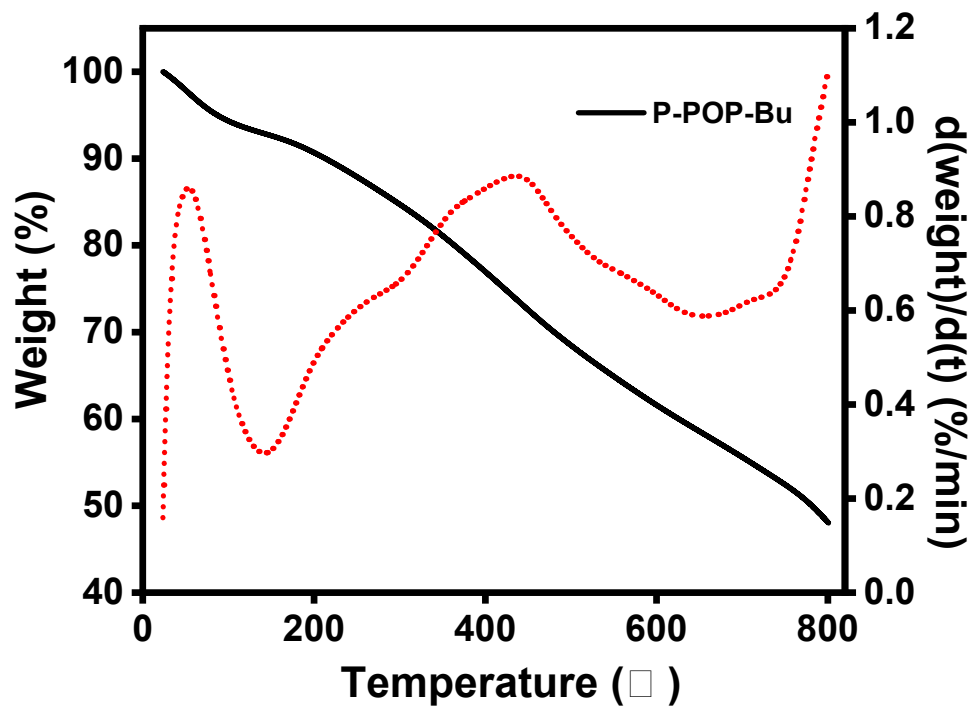


Figure S4. Temperature dependence of mass of P-POP-BU

Section 7. N₂ adsorption and desorption test and pore size distribution

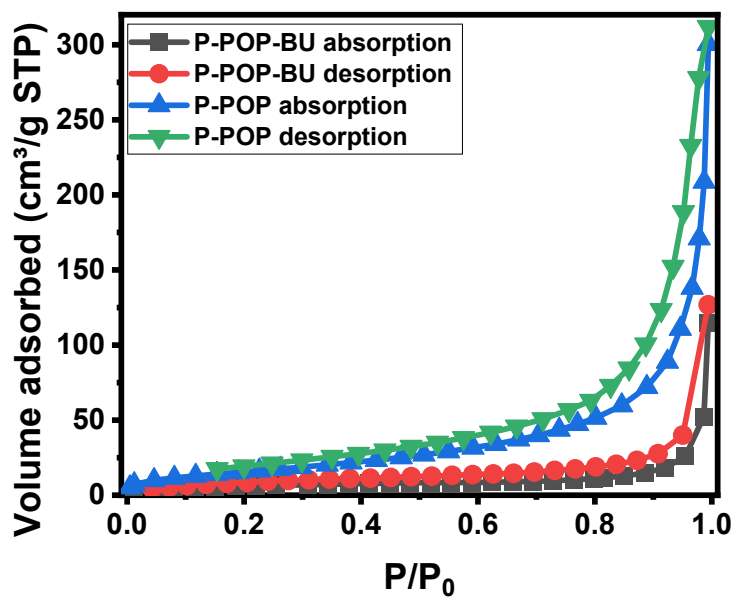


Figure S5. N₂ adsorption and desorption curves of P-POP-BU

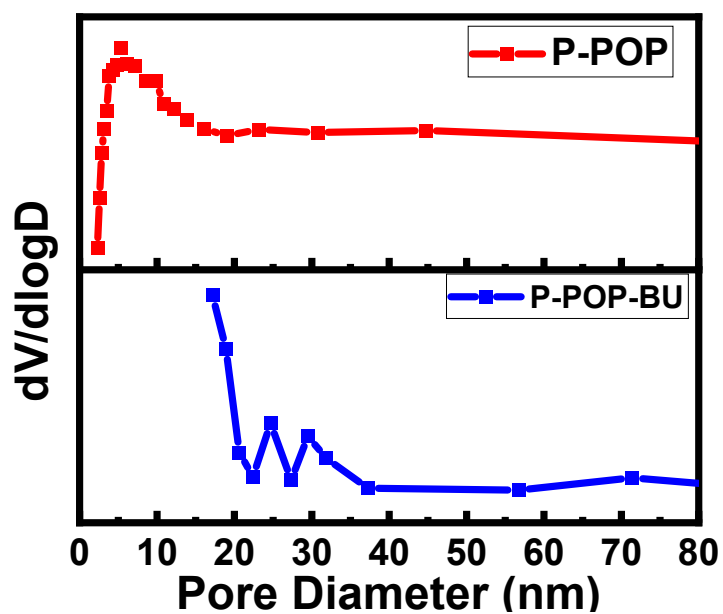


Figure S6. Pore size distribution of P-POP-BU

Section 8. Degradation of P-POP under different conditions

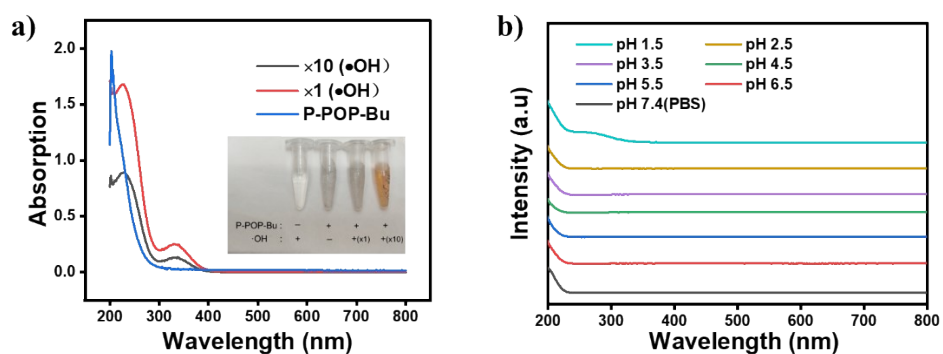


Figure S7. a) Degradation of P-POP at different OH concentrations; b) Degradation in PBS at different pH values

Section 9. MTT assay and hemolysis test for P-POP-Bu

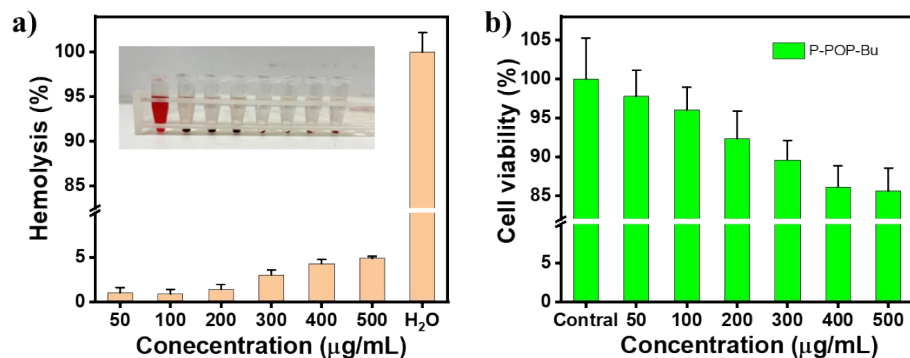


Figure S8. a) Effect of different concentrations of P-POP on the hemolysis rate of erythrocytes; b) Effect of different concentrations of P-POP on the viability of 3T3 cells.

Section 10. UV absorption spectra and working curves of Bu in ethanol

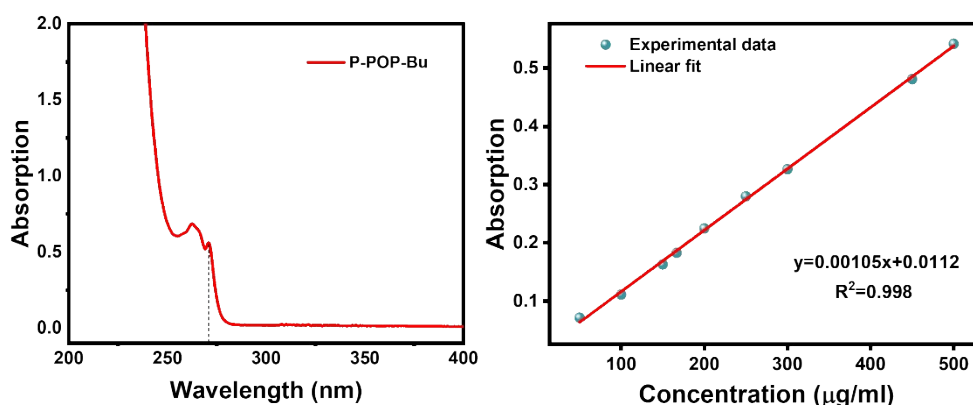


Figure S9. UV Absorption Spectra and Standard Curves of Bu in Ethanol.

Section 11. Working Curve of Bu in PBS and BU Release from P-POP-BU

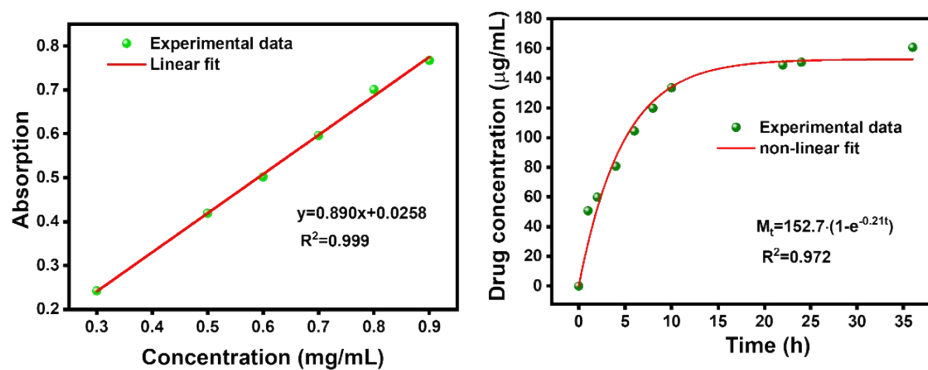


Figure S10. BU working curves in PBS and BU release from P-POP-BU in PBS over time.

Section 12. Supported Table

Table S1. Drug loading and encapsulation rates of P-POP-Bu

P-POP (mg)	Bu (mg)	LC (%)	EF (%)
1	2	35.82 ± 0.73	29.81 ± 2.15
1	4	58.83 ± 1.11	35.81 ± 1.65
1	6	66.95 ± 1.12	33.05 ± 1.18
1	8	70.79 ± 3.54	27.1 ± 1.49